2019 IEEE 4th International Conference on Advanced
Robotics and Mechatronics (ICARM)

Control of the Robotic Leg Prostheses Based on a Neuromuscular Model

Ming Pi, Yuxia Yuan and Zhijun Li

Abstract— **Traditional control method for prostheses is under the target locomotion and the known terrain conditions. The relationship between the torque and angle for each joint can be build from the measurements of normal human walking locomotion. Hence, these methods can not adapt to the different walking locomotion or the terrain variations. This paper presents an adaptive muscle-reflex controller, which utilizes the knee plantar flexor to comprise a Hill-type muscle to control the joint's movement. The parameters for controller were adjusted to fit the human knee's performance based on the Hill-type muscle model. Then, the experiments were conducted for the level ground walking, stair ascent walking and stair descent walking. For these experiments, it was observed that the powered prosthesis based on the neuromuscular controller can automatically adapt to the terrain variations, similarly to the normal human walking locomotion, without the known of the specific terrain variations.**

I. INTRODUCTION

Normal prostheses usually adopt the passive and lightweight structures to provide the elastic performance during the walking locomotion. To imitate the normal human walking performance, passive prostheses recycle certain energy stored when the dorsiflexion and plantar flexion were conducted and successively released for the next walking gait, just like the muscle-tendon complex did in the intact human walking [1], [2]. However, passive prostheses which approximate the joint's elastic performance can only behave during the slow walking. The additional powered energy is required for the normal and fast walking gaits [3]- [6]. Furthermore, these gaits are distinctly asymmetric. Compared with the unaffected side of amputee, the movement of knee joint on the affected side become smaller with the hip movement greater [7], [8]. Due to the greater power usage of hip joint to compensate for the usage of knee joint, greater metabolic energy was expended during the walking than nonamputees [9]-[13].

Hence, the powered robotic leg prostheses have been proposed for a normal and economical walking gait [14]. The powered prostheses mostly have comparable size and weight to the lower limb of intact human. Meanwhile, the novel elastic energy storage and extra motor power provide the natural daily walking activity. Some works have been explored for the control of powered robotic leg prostheses [15], [16]. In [17], the state profile between torque and angle of knee joint for the intact human has been build, to conduct the active movement to be performed. Different from the spring-like performance by the traditional passive prostheses, this powered robotic leg prostheses can support the faster walking locomotion in certain terrain condition. However, this control method can not adapt to the terrain variations. Actually, the controller in [17] required the intended locomotion under certain walking terrain.

In this paper, an adaptive controller based on a neuromuscular model has been proposed, which can produce the positive force feedback control for the movement of knee joint. Actually, the controller for the knee joint is combined with two actuators. For the movement of plantar flexion, the actuator is constructed based on a Hill-type muscle model to produce a positive force feedback control to mimic the natural reflexive muscle response for the knee joint. For the movement of dorsiflexion, the actuator is constructed as impedance controller to perform as a virtual rotary spring-damper.

II. METHODS

A. Robotic Leg Prosthesis

The mechanical design of the robotic leg prosthesis is shown as Fig. 1. The robotic leg prosthesis consisting of 2-DOF powered joints has been designed and optimized.

*This work was not supported by any organization

M. Pi and Z. Li are with the Department of Automation, University of Science and Technology of China, Hefei 230027, China (e-mail: piming1987@outlook.com; zjli@ieee.org).

Y. Yuan is with the Department of Automation, South China University of Technology, Guangzhou 510000, China (e-mail: yuxia.yuan2@outlook.com).

978-1-7281-0064-7/19/$31.00 ©2019 IEEE

The proposed robotic leg prosthesis can be detailed from the following sections: the mechanical design, the sensor design, and the control system design. The structure of the prosthesis is constructed from 3D-printing with the aluminum alloy and the nylon fiber. The mass of the proposed prosthesis is 4.8 kg, similar to a normal healthy limb. The weight distribution of prosthesis is presented as Table I. The prosthesis is constructed with two joint motors which can be driven respectively, with the flexion about 120° for the knee joint and planterflexion about −45° and dorsiflexion about 25° for the ankle joint. The leg joint is driven by Maxon EC45 Powermax brushless motor, which can be capable of 90 W for the continuous power. The ankle executing agency for the prosthesis is provided by the two-link structure for the sagittal plane, via the rotating pair to drive the ankle joint respectively. The length of the prosthesis can be changed by adjusting the length of two parts: the coupler from the ball nut to ankle, and the pyramid connector which couples the prosthesis to the socket of the amputee. The design specifications are presented in Table II. There have two revolute joints for the proposed prosthesis. The joint power specifications required for the prosthesis are based on the 61 kg amputee for a walking speed of 80 steps/min under walking level ground. Each revolute joint is driven by Maxon dc motor, EC45. The servo driver Elmo controls the Maxon EC45 Power Max brushless motors, which are connected to a personal computer via CAN bus. The position, velocity and torque signals of joints can be get from the servo motors in real time, sampling at 1 kH. An application interface developed by visual C++ language has been constructed for the all possible control strategies, monitoring signals and tuning controller parameters in real time. Moreover, the joints position, speed and output torque, et. al can be stored during the execution and analyzed off-line after the execution of control method. There have implemented three-level safety precautions in the mechanical, electrical and software designs. The mechanical limit of the knee and ankle can stop excessive movement of the prosthesis from an overstretch of the joints. Then, an emergency stop button is equipped to shut down the power supply for the system on emergency situations. At last, the motor current and other control parameters are limited by the command of interface program.

Fig. 1. Mechanical structure of the prosthesis [18]

TABLE I
MASS DISTRIBUTION OF ROBOTIC PROSTHESIS

Part	Mass(kg)	Weight
Body Structure	1.06	22%
Ankle Unit	0.91	19%
Knee Unit	1.01	21%
Electronics Assembly	0.38	8%
Carbon Fiber Foot	0.86	18%
Shell	0.58	12%
Total	4.8	100%

B. Control Structure

The control structure is designed to regulate the knee joint of the powered prosthesis to perform coordinately with the amputee's healthy leg under different terrain conditions. Based on the neuromuscular model for the knee joint of human, the controller generates the command torque for the movement of the powered prosthesis. The proposed controller includes two parts: neuromuscular activation and Hill-muscle model.

1) Neuromuscular Activation: Muscle activation dynamics is consist of neural activation dynamics and nonlinear relationship between neural activation and muscle activation. A second order critical damping system can be build to represent the

TABLE II
MECHANICAL CONFIGURATIONS

Configuration	Value
Total Weight	4.8 kg
Height of Knee Joint	0.40 m to 0.52 m
Motion Range of Knee	0° to 120°
Maximum Torque of Knee	80 Nm
Peak Power of Knee	90 W
Motion Range of Ankle	−45° to 25°
Maximum Torque of Ankle	100 Nm
Peak Power of Ankle	90 W

978-1-7281-0064-7/19/$31.00 ©2019 IEEE

manner of neural activation dynamics.

$$v(t) = \alpha s(t-d) - \beta_1 v(t-1) - \beta_2 v(t-2) \quad (1)$$

where $v(t)$ represents neural activation, $s(t)$ represents sEMG amplitude, d represents the electromechanical delay, and α, β_1, β_2 represent recursive coefficients.

Then we get

$$\begin{aligned} \beta_1 &= C_1 + C_2 \\ \beta_2 &= C_1 \cdot C_2 \end{aligned} \quad (2)$$

The recursive coefficients can be regulated as:

$$|C_1| < 1, \ |C_2| < 1 \quad (3)$$

$$\alpha - \beta_1 - \beta_2 = 1 \quad (4)$$

The nonlinear relationship between neural activation and muscle activation can be proposed as:

$$a(t) = \frac{s^{Au(t)} - 1}{s^A - 1} \quad (5)$$

where $v(t)$ represents neural activation, and A can adjust the degree of nonlinearity, which can be proposed in the range [-3,0]. If A equals 0, it's changed to be the linear relationship, and if A equals to -3, it's changed to be an exponential relationship.

2) Hill Muscle Model: The proposed controller is based on the Hill's muscle model, generating the muscle force command for the movement of knee joint. The muscle force is generated from the muscle reflexes, muscle activation, muscle fiber and the viscoelastic tendon. The muscle fiber is a contractile element in parallel with the elastic element. Then, The muscle force $F_i^{mt}(t)$ generated by the neuromuscular model can be described as:

$$F_i^{mt}(t) = F_i^{max}[f_i(l_i) f_i(v_i) a_i(t) + f_{pi}(l_i))] cos(\psi_i(t)) \quad (6)$$

where $F_i^{mt}(t) = F_i^t(t)$, $F_i^t(t)$ represents the tendon force, with $f_i(l_i))$ and $f_i(v_i)$ representing the force-length relation and the force-velocity relation of the contractile element, and $f_{pi}(l_i)$ represents the elastic tendon force-length relation, F_i^{max} represents the maximum generated force, l_i represents the muscle fiber length, and v_i represents the muscle fiber velocity.

Then, the contractile element can generate the force as $F_{at}^m(t) = f_i(l_i) f_i(v_i) a_i(t) F_i^{max}$, while, the parallel elastic element generates the passive force as $F_{pi}^m(t) = f_{pi}(l_i) F_i^{max}$. The pennation angle $\psi_i(t)$ can be defined as the angle from the tendon to the muscle fiber, and can be described as

$$\psi_i(t) = sin^{-1}\left(\frac{l_{oi}^m sin(\psi_{oi})}{l_i^m(t)}\right) \quad (7)$$

where $l_i^m(t)$ represents the length of muscle fiber and ψ_{oi} represents the optimal pennation angle with the optimal length of muscle fiber l_{oi}^m.

To simplify the calculation, we can get

$$f_i(l_i) = \begin{cases} q_0 + q_1 \cdot l_i + q_2 \cdot l_i^2 & 0.5 \le l_i \le 1.5 \\ 0 & otherwise \end{cases} \quad (8)$$

where $q_0 = -2.06$, $q_1 = 6.16$, and $q_2 = -3.13$ are set to be constants, and let $f_{pi}(l_i) = e^{10 \cdot l_i - 15}$, $f_i(v_i) = 1$.

As shown in the previous works, the optimal length of muscle fiber increases with the decrease of the muscle activation. Then, we can get the relationship between the optimal length of muscle fiber and the activation fluctuations as

$$l_{oi}^m(t) = l_{oi}^{'m}(\gamma(1 - a_i(t)) + 1) \quad (9)$$

where $l_{oi}^{'m}$ represents the optimal length of muscle fiber at its maximum activation, and γ represents the changed percentage at the optimal length of muscle fiber, which can be chosen as 15%.

As shown in the previous works, the tendon slack length l_{si}^t is bigger than the tendon length $l_i^t(t)$, with $l_i^t(t) > l_{si}^t$.

The model of tendon length can be assumed as

$$l_i^t(t) = l_i^{mt}(t) - l_i^m(t) cos(\psi_i(t)) \quad (10)$$

with $l_i^{mt}(t)$ representing the length of muscle tendon.

To simplify the analysis of Hill muscle model, we set the parameters $(F_i^{max}, \ l_i^t(t), \ l_{oi}^m, \ \psi_i(t))$ as constants. Then, the musculotendon length of $l_i^m(t)$ can be calculated from (10) and the musculotendon force from (6).

III. Experiment

A. Experimental Studies

In this section, we conduct two experiments on the robotic leg prothesis to verify the performance of the proposed controller under varying terrain conditions.

Fig. 2. Human-walking experiment under level ground

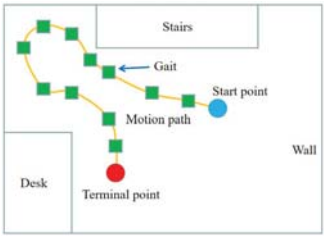

Fig. 3. Motion path under level ground

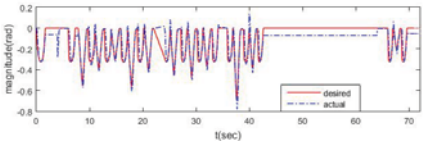

Fig. 4. Trajectory performance for knee joint under level ground

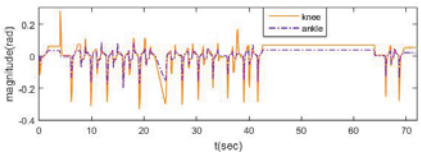

Fig. 5. Errors under level ground

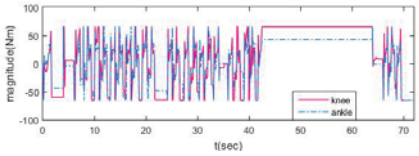

Fig. 6. Controller outputs of joints under level ground

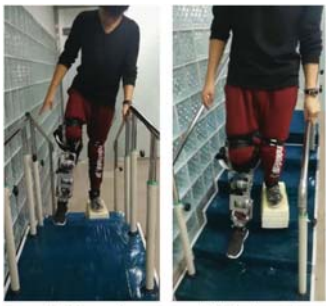

Fig. 7. Human-walking experiment under stairs

1) Case S1: The objective in this case is to verify the proposed control scheme for the robotic leg prosthesis under the level ground. The amputee with the prosthesis walks on the level ground for several steps in the room, as shown in Fig. 3. The user walks optionally in the room from the start point to the terminal point with a 180-degree turn. The experimental results with the prosthesis are shown in Fig. 4–Fig. 6. In Fig. 4, the tracking performance of the proposed controller was presented. The desired trajectories was shown in Fig. 4. The tracking errors was shown in Fig. 5. The controller outputs of joints was shown in Fig. 6. As shown above, the tracking errors tend to the zeros eventually. These experiment results show the theoretical performance of the proposed controller. The amputee can walk naturally on the level ground.

2) Case S2: The objective in this case is to verify effectiveness of the proposed control scheme for the robotic leg prothesis under the stairs ascent and descent. The stairs ascent have five steps. Each step has the height about 12 cm and the width about 28 cm. The stairs descent have six steps. Each step has the height about 10 cm and the width about 28 cm. There is a platform at the top of the stairs, with the length of 81 cm. The amputee with the prosthesis walks on the stairs ascent and descent. The experimental results with the robotic leg prosthesis for the knee joints are depicted in Fig. 8–Fig. 10 using the proposed approach. We can observe that the desired trajectories are nearly overlapping with the measured ones in Fig. 8. The tracking errors are presented in Fig. 9. The control signals are shown in Fig. 10. From the experiment results, we can see that the actual position trajectories converge to the desired trajectories. From these figures, conclusions can be drew that even if we have no knowledge of the stairs, the desired trajectories can still be obtained by the proposed control scheme.

IV. Conclusion

As the important performance of walking locomotion, the ability to adapt to different terrain

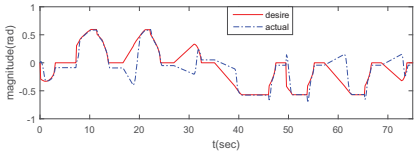

Fig. 8. Trajectory performance for knee joint under stairs

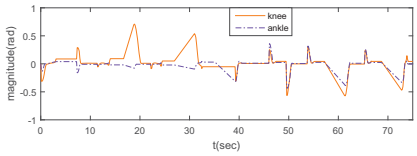

Fig. 9. Errors under stairs

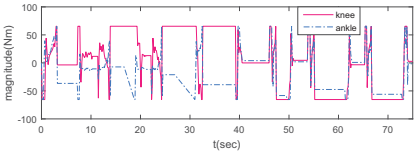

Fig. 10. Controller outputs of joints under stairs

conditions has been the key for the robotic leg prosthesis. However, the traditional passive prosthesis can not automatically transform to the different terrain conditions due to the lack of active power supply for the necessary normal gait. Hence, this paper presents an adaptive muscle-reflex controller, which utilizes the knee plantar flexor to comprise a Hill-type muscle to control the joints movement. The controllers parameters were adjusted to match the human knees performance based on the Hill-type muscle model. Then, the experiments were conducted for the level ground walking, stair ascent walking and stair descent walking. During these experiments, the adaptation of powered prosthesis based the neuromuscular controller was observed in response to the terrain variations, similarly to the normal human walking locomotion, without the explicit terrain sensing.

REFERENCES

[1] A. L. Hof, B. A. Geelen, and J. Van Den Berg, "Calf muscle moment, work and efficiency in level walking; role of series elasticity," *Journal of Biomechan*, vol. 16, no. 7, pp. 523–537, 1983.

[2] D. A. Winter, "Biomechanical motor pattern in normal walking," *Journal of Motor Behavior*, vol. 15, no. 4, pp. 302–330, 1983.

[3] M. Palmer, "Sagittal plane characterization of normal human ankle function across a range of walking gait speeds," *M.S. thesis*, Massachusetts Inst. Technol., Cambridge, MA, 2002.

[4] D. H. Gates, "Characterizing ankle function during stair ascent, descent, and level walking for ankle prosthesis and orthosis design," *M.S. thesis*, Boston Univ., Boston, MA, 2004.

[5] A. H. Hansen, D. S. Childress, S. C. Miff, S. A. Gard, and K. P. Mesplay, "The human ankle during walking: Implication for the design of biomimetic ankle prosthesis," *Journal of Biomechan*, vol. 37, no. 10, pp. 1467–1474, 2004.

[6] D. A. Winter and S. E. Sienko, "Biomechanics of below-knee amputee gait," *Journal of Biomechan*, vol. 21, p-p. 361–367, 1988.

[7] H. B. Skinner and D. J. Effeney, "Gait analysis in amputees," *American Journal of Physical Medicine and Rehabilitation*, vol. 64, pp. 82–89, 1985.

[8] H. Bateni and S. Olney, "Kinematic and kinetic variations of below knee amputee gait," *Journal of Prosthetics Orthotics*, vol. 14, no. 1, pp. 2–13, 2002.

[9] G. R. Colborne, S. Naumann, P. E. Longmuir, and D. Berbrayer, "Analysis of mechanical and metabolic factors in the gait of congenital below knee amputees," *American Journal of Physical Medicine and Rehabilitation*, vol. 92, pp. 272–278, 1992.

[10] R. L. Waters, J. Perry, D. Antonelli, and H. Hislop, "Energy cost of walking amputees: The influence of level of amputation," *Journal of Bone and Joint Surgery-American Volume*, vol. 58, no. 1, p. 4246, 1976.

[11] E. G. Gonzalez, P. J. Corcoran, and L. R. Rodolfo, "Energy expenditure in B/K amputees: Correlation with stump length," *Archives of Physical Medicine and Rehabilitation*, vol. 55, pp. 111–119, 1974.

[12] D. J. Sanderson and P. E. Martin, "Lower extremity kinematic and kinetic adaptations in unilateral below-knee amputees during walking," *Gait Posture*, vol. 6, pp. 126–136, 1997.

[13] A. Esquenazi and R. DiGiacomo, "Rehabilitation after amputation," *Journal of the American Podiatric Medical Association*, vol. 91, no. 1, pp. 13–22, 2001.

[14] S. K. Au, J. Weber, and H. Herr, "Biomechanical design of a powered ankle-foot prosthesis," in *Process of IEEE International Conference for Rehabilitation and Robotics*, Noordwijk, The Netherlands, Jun. 2007, pp. 298-303.

[15] S. Au, J. Weber, E. Martinez-Villapando, and H. Herr, "Powered ankle-foot prosthesis for the improvement of amputee ambulation," in *Process of IEEE International Conference for Engineering, Medicine and Biology*, Lyon, France, Aug. 23-26, 2007, pp. 3020-3026.

[16] H. Herr, J. Weber, and S. Au, "Powered ankle-foot prosthesis," in *Biomechanics of the Lower Limb in Health, Disease and Rehabilitation*, Manchester, U.K., Sep. 3-5, 2007, pp. 72-74.

[17] S. K. Au, "Powered ankle-foot prosthesis for the improvement of amputee walking economy," in *Ph.D. dissertation*, Massachusetts Inst. Technol., Cambridge, MA, 2007.

[18] Q. Li, S. Chen, C. Xu, and X. Chu, et al., "Design, control and implementation of a powered prosthetic leg," in *2018 11th International Workshop on Human Friendly Robotics*, Shenzhen, China, Nov. 2018, pp. 85–90.